Surface & Coatings Technology 447 (2022) 128837

Contents lists available at ScienceDirect

Surface & Coatings Technology

journal homepage: www.elsevier.com/locate/surfcoat

Cold spraying on polymer-based composites: Understanding the single-particle adhesion

Alessia Serena Perna *, Antonio Viscusi, Roberta Della Gatta, Antonello Astarita

Dept. of Chemical, Materials and Production Engineering, University of Naples "Federico II", P.le Tecchio 80, 80125 Naples, Italy

ARTICLE INFO

Keywords:
Cold spray depositions
Bonding mechanisms
Composites
Metal powders
Theoretical model

ABSTRACT

The metallization of the polymer matrix composite structures arises from the need to overcome some of the limits of the polymer-based materials, such as poor thermal and electrical conductivity. The cold spray technology has proved to be one of the most valid solutions for this scope. While the adhesion mechanisms of metal particles on metallic substrates are quite well known, the phenomena occurring when cold spraying on polymers are far to be understood. In this scenario, this paper proposes an interpretation of the phenomena leading to adhesion in cold spraying of metal particles onto polymer-based substrates, including composites. The aim is to try to unveil the phenomena ruling the adhesion by proposing a theoretical model conceived by conjecturing the phenomena occurring. The main hypothesis is that the adhesion is influenced by several energy-activated phenomena: the plastic deformation of the polymer, the plastic deformation of the particles and the loading of the fibers are conjectured to be the most influencing factors. So, the idea is to try to identify the most likely to occur phenomena based on an energy balance. A theoretical model is developed and validated through a dedicated experimental campaign to verify the effectiveness of the model to provide sufficiently reliable results. The model is applied to literature cases and the outcomes obtained are discussed to elucidate the adhesion mechanisms and the role of the fibers in fiber-reinforced polymers.

1. Introduction

Cold spray deposition is an intriguing coating technique that was firstly developed in the seventies [1] and which is finding an increasing interest in the last years in the whirlwind of additive manufacturing [2]. Briefly, the technique consists in accelerating a stream of metal particles by means of a carrier gas, then these particles impact against the substrate and, depending on the kinetic energy of the particles, different phenomena can be observed: rebounding when the energy is too low, erosion when the energy is too high, adhesion when the energy falls within a proper range [3]. The energy required to achieve adhesion is ruled by the properties of the particles and substrate [4], the interesting point of this technique is the possibility to process heat-sensitive materials [5], in fact both the particles and the substrate remain in solid state during the process, and the possibility to produce coatings of various metals on a large number of substrates [6].

A cornerstone in developing the cold spray deposition has been the understanding of the adhesion mechanism between the powders and the substrate and between the first layer of particles and the subsequent impinging particles [7]. To reveal these mechanisms different theories were proposed in literature such as interfacial restructuring [8] or amorphization [9], mechanical interlocking [10,11], oxide-layer breakup [12] and adiabatic shear instability [7,13] and several numerical models were also developed aiming to explain and interpret these intriguing adhesion phenomena [7]. Some points are still under debate, for instance, the adiabatic shear instability, which was the most accredited adhesion mechanism for CS [14], was proved to be not essential for coating formation from the last activities carried out by Hassani-Gangaraj et al. [11]. The question "which is the most prevailing adhesion mechanism?" still stands to date and several research groups are proposing their lesson.

All the above studies and theories are focused on the deposition of metal particles on metallic substrates, while the more recent trend in cold spray is the production of metallic coatings on polymeric substrates. In fact, some of the surface characteristics of polymers, included composites materials, such as electrical conductivity, thermal conductivity, electromagnetic shielding, erosion, radiation, and lightning protection can be improved through the surface metallization process. Several studies provided diverse successful depositions including titanium coating onto PEEK for a biocompatibility function of surgical implants [15], thin or thick copper coating onto various polymers such as

* Corresponding author.
E-mail address: alessiaserena.perna@unina.it (A.S. Perna).

https://doi.org/10.1016/j.surfcoat.2022.128837
Received 12 April 2022; Received in revised form 10 June 2022; Accepted 24 August 2022
Available online 31 August 2022

General symbols

a	radius of the contact surface between the substrate and the particle
a^*	radius of the contact area at the point of maximum compression
δ^*	penetration of the particle at the point of maximum compression
ΔE	difference between energy possessed by the particle and energy required for adhesion
ε_0	failure strain of the substrate
ε_s	substrate strain
E_f	elastic modulus of the fibers of the composite substrate
E_g	potential energy
E_k	kinetic energy
E_{load}	energy required for the loading of the fibers
E_m	elastic modulus of the matrix of the composite substrate
E_{pow}	elastic modulus of the powder material
$E_{PLA(s)}$	energy required to plastically deform the substrate
$E_{PLA(p)}$	energy required to plastically deform the particle
E_{pot}	internal potential energy
E_s	elastic modulus of the composite substrate
E_T	thermal energy
E_t	heath exchange between the particle and the substrate
f	degrees of freedom
g	acceleration of free fall
h	distance of the flying particle from the ground
H_c	thermal conductivity of the system
k_b	Boltzmann constant
k_f	fiber thermal conductivity
k_m	matrix thermal conductivity
k_p	particle thermal conductivity
k_s	substrate thermal conductivity
m	mass of the particle
m_s	mass of the substrate
N	number of molecules of a system
N_A	Avogadro number
P_0	air pressure measured at the inlet of the nozzle
p_d	mean contact pressure during dynamic loading
p_m	contact pressure in the contact surface between the particle and the substrate
ρ_p	powder particle density
r	radius of the particle
R	average radius of curvature in the contact area
r_1	semi-minor axis of the deformed particle
R_c	radius of the cone formed at the rear surface of the composite after the impact
s	space covered by the particle within the polymer
SoD	stand-off distance
t	time necessary for the particle to adhere
T	composite thickness
T_p	particle temperature
T_s	substrate temperature
v	impact velocity of the particle
v_g	carrier gas velocity
V_s	volume of a spherical particle
x	the axial position of the particle in the nozzle
Y_p	yield stress of the particle material
Y_s	yield stress of the substrate material

silicone, PVC, epoxy substrates, PU, HDPE, PP, nylon 6 and PTFE for antifouling function of marine engines [16], electrical conductive capability for electronic devices [17], lightning strike resistance of aeronautic structures [18] and so forth for several engineering applications [19]. Particularly for aeronautical and aerospace fields, polymer-based structures due to their unique properties, such as their combination of low density and high mechanical performances, can replace metallic materials in many applications, such as aircraft

Table 1
Literature reports of cold spray depositions of metallic powders on composite substrates.

Sprayed Particles	Target Surface		Deposition parameters					Literature references	
Powders Typology	Matrix Material	Fiber typology	Carrier Gas	Carrier Gas-Pressure, P [bar]	Carrier Gas-Temperature, T [°C]	Nozzle- speed [mm/s]	SoD [mm]	Best cases	Reference
Al.	Epoxy resin	Glass fibers	.Air	5–30	room temperature	8.3	40	P = 5 bar	[20]
Al, Al/Cu	PEEK450 CA30	Carbon-fibers.	.Nitrogen	12–19.	300–450.	5	15–20	Powders = Al-Cu P = 19 bar T = 450 °C SoD = 15 mm	[21]
Al	Airplane Grade Epoxy	Carbon fibers	Nitrogen	5–20	300–600	200	20	P = 5 bar T = 600 °C	[22]
Al, Cu, Sn, Sn/Zn	Epoxy resin	Carbon fibers	Nitrogen	2.9–50	25–700	12.5–500	18–200	Powders = Sn-Zn P = 5.5 bar T = 300 °C	[23]
Cu	Epoxy resin	Carbon fibers	Nitrogen	20	250–425	1000	40	T = 425 °C	[24]
Cu, Sn, Fe	Epoxy resin	Carbon fibers	Nitrogen	3–49	200–425	25	18–40	Powders = Sn P = 12 bar T = 200 °C	[25]
Sn, Sn/Cu, Sn/Zn	Epoxy resin	Carbon fibers	Nitrogen	4.1–6.9	280–350	25	18	T = 300 °C P = 4.1 bar 10Cu	[26]
Al	Polylactic acid (PLA) films	Hemp fibers-	Air	4–8	150–600	3	10–80	P = 6 bar T = 200 °C	[27,28]
Al/Al_2O_3	Polylactic acid (PLA) films	Hemp fibers	Air,	7.	200	3.	50.	%(Al_2O_3) = 30 wt%	[29]

structures. The main limitations for such applications are their electrical resistance. The aircraft structures need to be electrically conductive to avoid damage from lightning strikes and thunderstorm electric field attacks.

The adhesion between metallic particles and polymeric substrates, in cold spray, has been widely experimentally observed and an increasing number of papers is available in the literature. Table 1 summarizes the main powder/substrate configurations investigated, and the relative process parameters adopted.

Looking at the table, the first point that leaps to the eye is that completely different process parameters for the same powder/substrate combinations have been proposed, some authors for instance investigated pressure ranges from 4 to 50 bars. This emphasizes the lack of a single vision in the literature about the best process parameters and equipment to use for an effective deposition. It is possible to highlight that very different approaches have been used, this suggests that the mechanisms ruling the adhesion are not known, so a trial-and-error approach is used instead of one based on theoretical considerations. In any case, some preliminary considerations can be drawn from the literature survey carried out. The polymer matrix typology (e.g., whether the polymer matrix is thermoplastic or thermosetting), for example, was proved to be very influential on the particle impact phenomena. In this regard, Ganesan et al. [30] examined the effect of the typology of substrate chosen on the bonding mechanism of the particle and concluded that the particles will bond with the surrounding polymer matrix only when they penetrate the thermoplastic substrate profoundly. On the contrary, the fragile behavior of thermosetting substrates makes coating formation and growth difficult, if not impossible. Moreover, Gillet et al. [31] observed that the deposition of powders also depends on the thickness of the polymer surface layer. The lay-up sequence and stratification and the fiber typology can also contribute to the effectiveness of CS depositions, as detailed by Viscusi et al. [32]. So, these outcomes should be considered in approaching the problem.

The main purpose of this work is to provide an interpretation of the complex phenomena occurring when metallic particles are impinged onto polymer-based substrates through cold spray, trying to unveil the physical mechanisms ruling the adhesion of metal particles on polymers. To this aim, an interpretative model for the impact of a single metallic particle on a polymeric substrate will be proposed and then validated with the experimental results.

The basic idea is that adhesion mechanisms are not mutually exclusive and, therefore, more than one phenomenon may take place during particle/substrate interaction. It is also assumed that all the mechanisms involved must require a certain amount of energy to take place. Therefore, an energetic approach is proposed in this work based on the evidence that the kinetic energy, once the particle has adhered to the substrate, is completely converted into other energy forms. It is also evident that, after the impact, several phenomena take place and the energy required for the adhesion is, therefore, equal to the total energy required for those phenomena to occur. In conceiving this model, the authors identified some energy activated phenomena that are likely to occur in cold spray, so the model is conceived as an equilibrium equation between the available energy and the energy requested to activate the hypothesized phenomena. A representative scheme describing the energy conversions hypothesized to occur during the deposition is presented in Fig. 1.

To summarize, the model has been conceived on the phenomena that the authors believe to occur during the deposition and rule the deposition itself (as reported in Fig. 1). The energy was chosen as interpretation key on the assumption that the above-hypothesized phenomena are energy activated, and two main questions have been posed: i) how much energy is required to activate these phenomena? ii) where does the kinetic energy of the particles go after the adhesion occurs? In the authors' opinion, if we can answer these two questions, we are able to understand which are the involved phenomena. Moving one step ahead we could dare to suggest a theory: if the kinetic energy dissipated by the particles and the energy required to activate all the hypothesized phenomena are of the same order of magnitude, it is reasonable to be convicted that these are the ones responsible for the adhesion (adhesion that has been experimentally observed, let our recall).

The proposed model was calibrated through a dedicated experimental campaign, by comparing the outcomes of the model with the experimental pieces of evidence, once again testing the hypothesis done on the benchmark of the real deposition. After that, some experimental outcomes reported in the literature were discussed in the light of the proposed model to assess its capability to describe the adhesion process.

Summarizing this paper aims to answer several open issues: (i) which are the mechanisms/phenomena involved in the CS deposition on polymer-based materials; (ii) which is the role of the reinforcement when spraying on composites; (iii) which are the energy-related aspects

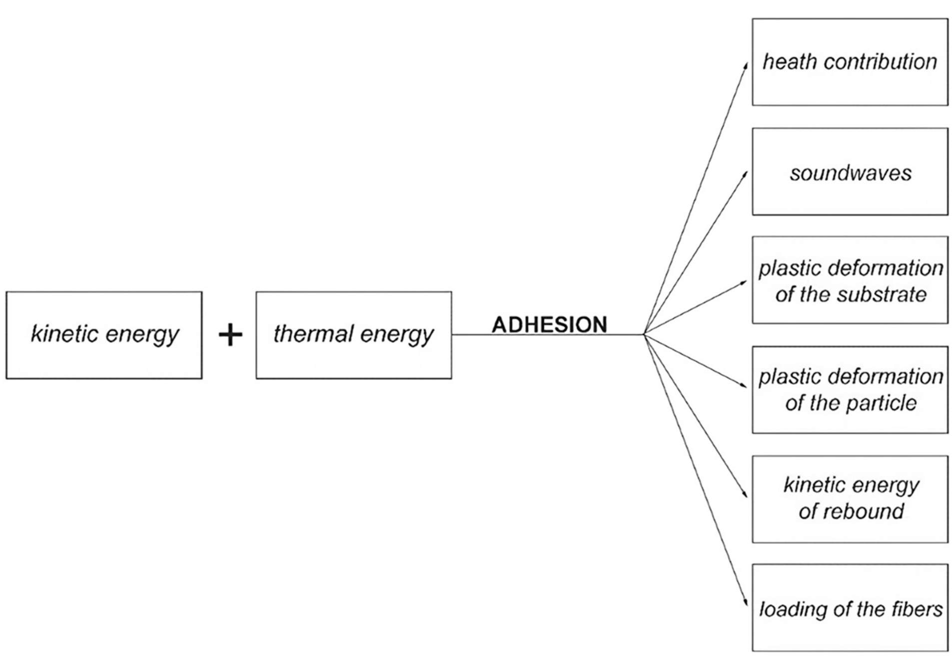

Fig. 1. Representative scheme describing the energy balance.

in CS on composites.

2. Model development

It is worth recalling that two different interactions can be observed in cold spraying: i) particle-to-particle interaction, which is responsible for the coating growth and ii) particle-to-substrate interaction which is responsible for the coating adhesion [33]. The present paper is focused on the latter interaction to shed light on the phenomena ruling the adhesion between the single particle and the target surface.

Two different energies can be defined: E_p, which is the amount of energy possessed by a single particle impacting the substrate and E_a, which is the amount of energy required to activate the phenomena (as conjectured by the authors) leading to the adhesion of the particle.

2.1. Calculation of E_p

The amount of energy owned by a particle (E_p) can be summarized as in Eq. (1).

$$E_P = E_k + E_g + \left(E_T + E_{pot}\right) \tag{1}$$

It is possible to define the kinetic energy of the particle as $E_k = \frac{1}{2}mv^2$. The potential energy can be written as $E_g = \text{mg}(h - h_0)$. The term $h\text{-}h_0$ corresponds to the stand-off distance, which is usually low in cold spray, as shown in Table 1. The average thermal energy of a system composed of N molecules having f degrees of freedom is $E_T = N\frac{f}{2}k_bT_p$ [34]. The internal potential energy relative to the molecules mutual position (E_{pot}) can be considered a constant value before and after the adhesion of the particles onto the substrate and it can be neglected in this study. Moreover, E_g can be assumed to be negligible if compared with the average values of E_k and E_T.

Therefore, based on the considerations above reported, Eq. (1), can be written as in Eq. (2), that is the energy possessed by a single particle moving toward a target surface in cold spraying.

$$E_p = \frac{1}{2}mv^2 + N\frac{f}{2}k_bT_p \tag{2}$$

2.2. Calculation of E_a

The main forms of energy in which the particle energy can be converted after the impact include (see Fig. 1): i) heat transfer contribution; ii) soundwaves; iii) plastic deformation of the substrate; iv) plastic deformation of the particle; v) kinetic energy related to the rebound of the particle. Regarding composite materials, due to the presence of the fibers, a further contribution must be taken into account: vi) loading of the fibers. In the following sections, the abovementioned contributions are discussed individually.

2.2.1. Heat transfer contribution

The particle transfers heat to the substrate by thermal conduction, by virtue of the temperature acquired during the process. Once it has impacted the substrate, the particle exchanges the acquired heat with the substrate by thermal conduction. The thermal flow is given by law (Eq. (3)), where T_p and T_s are the temperatures of the particle and the substrate, respectively.

$$q_c = H_C\left(T_p - T_s\right) \tag{3}$$

For a spherical particle having the r radius and exchanging heath with a lamina [35], $H_C = 4r \bullet (1/k_p + 1/k_s)^{-1}$, with k_p and k_s that are the thermal conductivities of the particle and the substrate, respectively.

The range of interest for the evaluation of the thermal exchange is the time the particle takes to adhere to the substrate, supposing to consider the particle adhered once it has reached its final position into the substrate, and therefore when its speed is zero. Neglecting the rebound effects, the time taken by the particle to adhere is $t = 2s/v$. It was assumed that the motion of the particle through the substrate is uniformly decelerated since the space covered is so short that other types of dissipative effects can be neglected. Therefore, the heat exchanged in this time interval is portrayed in Eq. (4).

$$E_t = \frac{H_c\left(T_p - T_s\right)2s}{v} \tag{4}$$

2.2.2. Soundwaves and elastic waves

During the elastic impact, if the velocity is small compared to elastic wave speeds, the quasi-static approach is justified, and the elastic waves can be neglected. Moreover, as assessed by Johnson in Contact Mechanics [36], this is further validated when plastic deformation occurs: in fact, the plastic flow leads to the dissipation of part of the energy, as it diminishes the intensity of the contact pressure, hence reducing the energy converted into elastic wave motion.

2.2.3. Energy absorbed due to plastic deformation of the substrate

Up to moderate impact speeds (about 500 m/s), the knowledge of inelastic impact under static conditions, following Hertz's theories, was used to analyze the impact behavior under a dynamic load. The decision to follow those theories is motivated by the energy absorption caused by the plastic flow. In order to analyze the energy absorbed in these conditions, the following assumptions have been made on the basis of the work of Johnson [36]: i) Yields are calculated with Tresca criterion for the sake of simplicity, as the results are not largely different compared to more complicated criteria. ii) Work hardening has been neglected. This assumption is acceptable due to the material and the field of tension that arises: in fact, as known from literature, the resulting deformation of the particle has to be considered small, hence the material does not show an interesting amount of work hardening [30]. iii) The impact of the particle is assumed to be normal to the substrate.

Under those conditions, assuming the fully plastic regime, the material does not pile-up or sink in along the edges of the impacting particle.

The kinetic energy consumed for the elastic and plastic local deformation of the impacting bodies (the particle and the substrate in this case), up to the instant where the compression reaches its maximum value, can be written as in Eq. (5).

$$\frac{1}{2}Mv^2 = \int_0^{\delta^*} P d\delta \tag{5}$$

where $\frac{1}{M} = \frac{1}{m_s} + \frac{1}{m}$.

In the case of a contact of a sphere with a substrate, the compressive load is $P = \pi a^2 p_m$. Assuming that the impact between the bodies results in purely plastic deformation, the energy absorbed by the substrate during deformation is portrayed in Eq. (6), where a^* is the radius of the contact surface between the substrate and the particle, p_d is the mean contact pressure during dynamic loading and R is the average radius of curvature in the contact area.

$$\text{EPLA}(s) = \int_0^{a^*} \pi a^2 p_d \left(\frac{a}{R}\right) da = \frac{\pi a^{*4} p_d}{4R} \tag{6}$$

The quantity $\pi a^{*4}/4R$ is the apparent volume of material displaced by the particle. It can be assumed that p_d is approximately equal to p_m being in the fully plastic regime, and its value is then $p_m = p_d = 3Y_s$ (which is the yield stress of the substrate material).

2.2.4. Kinetic energy related to the rebound of the particle

This quantity, which is not a material property but depends on the severity of the impact, can be neglected as a significant amount of energy is dissipated in the form of plastic deformation such that as the speed at initial impact increases, the coefficient of restitution decreases [37]. Moreover, under the hypothesis of achieving adhesion between the particle and the substrate, the rebound can be considered absent.

2.2.5. Energy absorption on account of the plastic deformation of the particle

The energy absorbed for the deformation of the particle was evaluated considering the ideal deformation firstly described by Dieter and Bacon [38]. Upon impact, the particle deforms, taking up an elliptical configuration, as shown in Fig. 2, due to the contact pressure. Assuming that the particle impact direction is perpendicular to the substrate, its radius in the impact direction contracts, becoming the semi-minor axis of the ellipse. The work required to deform the particle is expressed in Eq. (7).

$$\mathrm{dL} = \frac{3}{4}\left[-Y_p V_s \frac{dr}{r}\right] \Rightarrow \mathrm{E}_{PLA(p)} = \frac{3}{4} Y_p V_s ln\frac{r}{r_1} \tag{7}$$

2.2.6. Loading of the fibers

A theoretical model to evaluate the energy absorbed by a polymeric composite during ballistic impact was proposed by Morye et al. [39]. Given the velocities considered and the compatibility of the hypothesis, it was assumed in this research work that this model could be considered valid in the framework of cold spray. The following hypotheses have been made in the development of the model: i) the impacting body is rigid and does not deform during the impact; ii) the delamination causes a negligible absorption of energy; iii) the composite failure mechanism over the thickness is uniform; iv) the loss of energy spent to overcome the friction between the composite and the impacting body is insignificant and the subsequent heath production is negligible.

The model assumes that there are three main contributions to energy absorption: i) energy absorbed to promote the breaking of the strained fibers that have reached the tensile failure upon impact, E_{TF}. ii) Energy absorbed to deform the fibers that the impinging body has not impacted directly, E_{ED}. The propagation of transverse waves after the impact of the projectile, causes the yarns to deform and the formation of a cone in the rear surface of the composite. iii) The kinetic energy absorbed by the amount of the substrate that is put into motion by the projectile, E_{KE}. The total energy can be therefore written as in Eq. (8).

$$E_{Total} = E_{TF} + E_{ED} + E_{KE} \tag{8}$$

In cold spray, the particles inside the deposition window should not break the fibers, either put into motion a portion of the composite, due to their small dimension compared to the substrate. Therefore, the contribution of E_{KE} and E_{TF} can be considered negligible, in other words, it can be said that these contributions must be nihil when proper processing conditions have been set.

As for E_{ED}, it can be seen from Fig. 3 a schematic deformation of yarn upon the impact, where the radius of the abovementioned cone formed in the rear surface of the substrate is R_c.

The energy absorption during deformation can be evaluated by integrating the portion of the stress/strain curve of the composite at a given strain (namely, ε). Being this curve approximately linear for a composite material, it is possible to assert that (Eq. (9)):

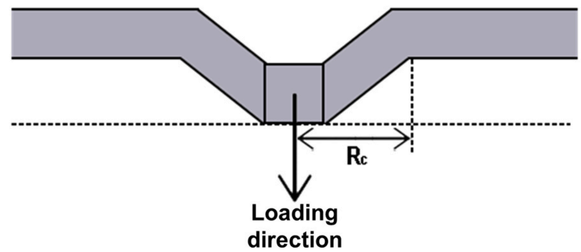

Fig. 3. Schematic side view of a fiber in a composite deformed during a ballistic impact.

$$E_{ED} = E_{load} = \frac{1}{2} E_s \varepsilon_s{}^2 \tag{9}$$

Depending on the impact point, not all the yarns deform in the same manner: the yarns closer to the impact point experience a strain close to their failure strain, while the farther ones likely do not strain at all. It can be then asserted that the strain of the composite can vary from a value $\varepsilon_s = \varepsilon_0$, equal to the failure strain of the composite at the impact point, to a value of $\varepsilon_s = 0$ at the R_c distance, where the yarn is undeformed. It is possible to express the variation of strain with Eq. (10)

$$\varepsilon = \frac{2(R_c - \mathrm{r})}{2R_c - 2r}\varepsilon_0 \tag{10}$$

and thus calculate the energy absorbed during deformation as in Eq. (11), where E_s is the elastic modulus of the composite substrate, T is the composite thickness and R_c is the radius of the cone formed at the rear surface of the composite after the impact.

$$E_{load} = \frac{\pi E_s \varepsilon_0^2 T}{(2R_C - 2r)^2}\left[\frac{R_C^4}{3} - \frac{(2r)^2 R_C^2}{2} + \frac{r^3 R_C}{3} - \frac{r^4}{16}\right] \tag{11}$$

2.3. Model formulation

Based on the considerations above discussed, it can be asserted that the main energy contributions for adhesion, shown schematically in Fig. 4, are: i) Heat contribution; ii) Plastic deformation of the substrate; iii) Plastic deformation of the particle; iv) Loading of the fibers. The assumptions on which this model is based can be here summarized: i) the energy spent to overcome the frictional force between the particle and the substrate is considered negligible; ii) the failure mechanism of the substrate is uniform along the thickness direction; iii) delamination causes a negligible absorption of energy; iv) a quasi-static approach has been chosen to describe the deformation of the surface; v) Yields calculated with Tresca criterion; vi) work hardening has been neglected.

At this point, a first formulation of the model can be released in Eq. (12), which describes the transformation of kinetic and thermal energy of the system to other energy contributions.

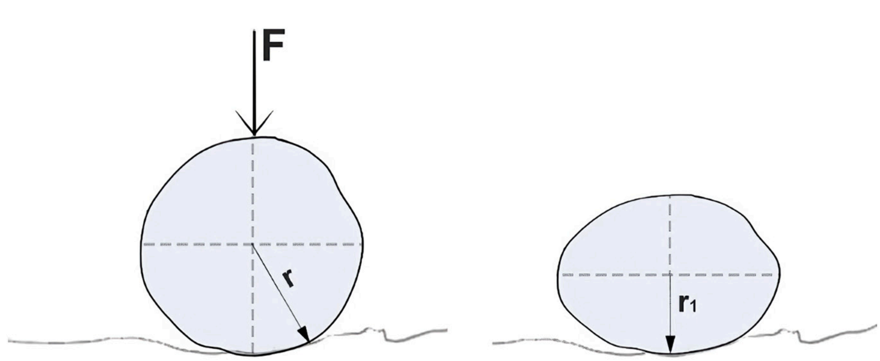

Fig. 2. Deformation of a single particle upon impact. *F* is the compressive force applied to the particle.

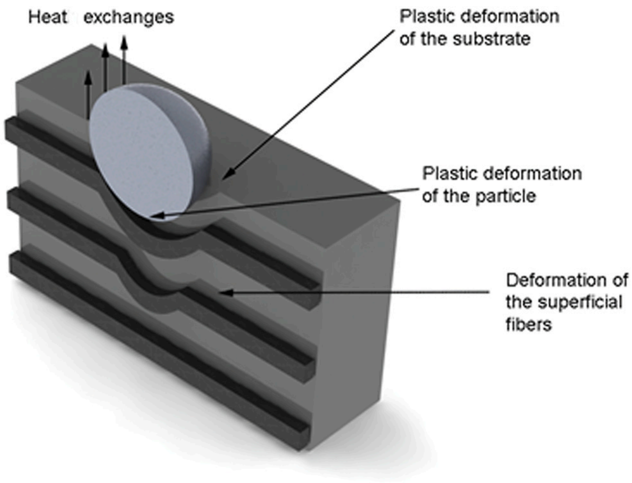

Fig. 4. Schematic description of the main energy contribution to the bonding in CS process.

$$\frac{1}{2}mv^2+N\frac{f}{2}K_BT_p=\frac{H_c(T_p-T_s)2s}{v}+\left(\frac{\pi a^{*4}3Y_s}{4R}\right)+\left(\frac{3}{4}\bullet Y_P\bullet V_s\bullet ln\frac{r}{r_1}\right)+\frac{\pi E_s\varepsilon_0^2T}{(2R_C-2r)^2}\left[\frac{R_C^4}{3}-\frac{(2r)^2R_C^2}{2}+\frac{r^3R_C}{3}-\frac{r^4}{16}\right] \quad (12)$$

In this formulation an issue arises: the contributions of particle deformation, substrate deformation and fiber loading are overestimated (as they have a mutual influence) and a distribution of the available energy (E_p) among these three contributions depending on the material properties is not considered. All these three contributions have a mutual influence which is dependent on the materials under investigation. For example, if steel powders are sprayed on a soft polymer (namely, a polymer characterized by low values of stiffness) it can be argued that the particle deformation will be almost zero while the polymer will experience a high deformation [40], while if softer aluminum particles are sprayed on a high-performance polymer (PEEK for instance) a deformation of both particles and substrate is expected and observed [41]; since E_p is constant, it can be assumed that the higher the deformation of the substrate the lower the deformation of the particle. On these premises, a coefficient accounting for the distribution of deformation between particle and substrate and depending on the material properties must be included. The coefficients A, B and C, as defined in Eq. (13), are therefore included in the model, where E_{pow} is the elastic modulus of the powder material, E_s is the elastic modulus of the composite substrate and E_f and E_m are the elastic moduli of the fibers and the matrix of the composite material, respectively.

$$A+B+C=1$$
$$\frac{A+C}{B}=\frac{E_{pow}}{E_s} \quad (13)$$
$$\frac{A}{C}=\frac{E_f}{E_m}$$

The final formulation of the model is reported in the *Vi-Pe-R-A* equation (Eq. (14)):

$$\frac{1}{2}mv^2+N\frac{f}{2}K_BT_p=\frac{H_c(T_p-T_s)2s}{v}+A\left(\frac{\pi a^{*4}3Y_s}{4R}\right)+B\left(\frac{3}{4}\bullet Y_P\bullet V_s\bullet ln\frac{r}{r_1}\right)+C\frac{\pi E_s\varepsilon_0^2T}{(2R_C-2r)^2}\left[\frac{R_C^4}{3}-\frac{(2r)^2R_C^2}{2}+\frac{r^3R_C}{3}-\frac{r^4}{16}\right] \quad (14)$$

3. Materials and methods for experimental validation

The theoretical model proposed through the *Vi-Pe-R-A* equation has been validated considering two different experimental cases: i) deposition of aluminum particles on unreinforced polymeric substrates and ii) deposition of aluminum particles on fiber reinforced polymers (FRP). For this purpose, sheets of polypropylene (PP) with a thickness of 0.25 mm were chosen for both the polymer-based substrates. Carbon fiber fabrics with an areal density of 220 g/m^2 were used as reinforcement for the composite material. The compression molding technique under a pressure of 1.1 MPa at 210 °C for 15 min was used for the manufacturing of both the panels' typologies. The curing temperature was set in accordance with the melting temperature of the polymer. The mold was cooled down in air, while the pressure was kept constant. The laminates so manufactured presented a thickness of approximately 2.5 mm. The choice of using these materials is due to the relatively high amount of material data available to the authors.

Micron-sized AlSi10Mg aluminum powders, provided by LPW South Europe and with a particle mean diameter of 30 μm and a spherical shape [42], were cold sprayed through a low-pressure equipment (DYCOMET). Air was used as carrier gas. Based on preliminary experimental tests and literature background [43,44], the inlet gas pressure and the SoD were set to 6 bar and 25 mm, respectively, and kept constant during all the depositions. Different tests were carried out by varying the gas inlet temperature, from 150 °C to 550 °C, to obtain different particles impact velocities, which increase as the gas temperature increases [45]. A k-type thermocouple was used to measure the gas temperature at the exit of the nozzle with the probe aligned with the axis nozzle. This allowed for identifying three different deposition ranges: i) a range of low impact velocity for which the particles do not have enough energy to adhere, with the resulting rebounding phenomenon; ii) a range of higher impact velocity where some particles start to adhere, and the deposition efficiency starts to increase; iii) a range of a further higher impact velocity with the particles that are well anchored to the substrates to form the coating. The streamwise jet velocity for a given gas temperature was measured by means of an hot-wire anemometer (Dantec Dynamics, MiniCTA, Skovlunde, Denmark), equipped with a 5 μm diameter, 1.25 mm long wire probe, and placed at the exit of the nozzle. Its output signal was acquired by the same data-acquisition system used to generate the electric signal, with a sampling rate of 10 kHz, for 2000 operating cycles. An estimation of the experimental uncertainty of the hot-wire data has been made following Yavuzkurt's work [46]. The uncertainty in the phase-averaged streamwise velocity is found to be <3 % for all the measured values.

It is worth noting that for these measurements, the particles were not injected into the nozzle so avoiding that the powders would cause damages to the anemometer probe.

In one-dimensional numerical models about particle acceleration by the high-speed gas, the particle velocity can be calculated by a drag force on a single particle in a fluid flow. In particular, Alkhimov et al. [47] obtained an empirical equation which includes the particle velocity, the gas velocity and the gas pressure. That means once the gas velocity was characterized, the resulting particle velocity at the exit of the nozzle can be calculated through the equation suggested in the literature [48] and reported in Eq. (15). Here, v is the particle velocity, P_0 is the air supply pressure at the entrance of the nozzle, ρ_p is the particle density, r is the particle radius and x is the axial position of the particle within the nozzle. The reliability of the proposed equation to make an effective prediction of particle velocity at the nozzle outlet under the investigated CS conditions was proved in the literature [47].

$$v=\frac{v_g}{1+0.85\sqrt{\frac{2r}{x}}\sqrt{\frac{\rho_p v_g^2}{P_0}}} \quad (15)$$

The adhesive strength of the particles after cold spray deposition was measured following the ASTM D4541 standard and by using a PosiTest

ATM. Aluminum dolly with a 10 mm diameter was bonded on the top surface of the cold sprayed deposits using cyanoacrylate glue, as shown in Fig. 5. Any excess adhesive or coating surrounding the dolly was removed with a drill bit.

Based on both the visual inspections and the results from the adhesive tests, three average values of the particles impact velocity for each deposition range above discussed were identified. The mean adhesion values, measured from 3 specimens coated employing the same deposition parameters, are illustrated in Fig. 6.

It is possible to observe that no adhesion occurred for the lowest impact velocities (100 m/s and 225 m/s for unreinforced and reinforced panels, respectively); moreover, the adhesion values measured on reinforced panels are slightly lower than the values obtained for the unreinforced specimens considering the same experimental conditions, in agreement with the literature results [49,50].

In summary, the experimental validation of the model was carried out following this procedure: firstly, the particle velocity value calculated from Eq. (15) was implemented into the *Vi-Pe-R-A* equation, then, the difference between the first member of the equation, representing the energy possessed by the particle before the impact, and the second one, which is the energy that the particle requires to adhere to the substrate, was calculated. Three possible cases were found: i) the difference is negative meaning that no adhesion should occur; ii) the first member equals the second one or it is a little above meaning that adhesion is expected; iii) the difference is positive meaning that the particle should have the proper energy to anchor with the substrate. Nevertheless, it is important to notice that the model relies on simplifying hypotheses and several dissipation phenomena are neglected; for this reason, the energy required for adhesion should be slightly higher than the quantity defined through E_a in the *Vi-Pe-R-A* equation. The authors will consider the model validated if it will be able to produce sufficiently converged results compared with the experimental deposition outcomes.

The main parameters required for the implementation of the model have been collected from the data sheets of the materials employed in the experimental tests and from literature, where necessary. It is worth to notice that several parameters required some experimental measurements and calculations based on commonly known material mechanics theories or isentropic flow models, which are not shown here for the sake of brevity. It was also assumed that: i) the substrate is at room temperature due to the relatively short time of deposition and ii) the particle reaches the same temperature of the carrier gas at the exit of the nozzle [51,52], so its properties have been evaluated at the gas temperature. All the involved parameters are reported in Table 2.

4. Results

4.1. Model validation

The results given from the model proposed in the *Vi-Pe-R-A* equation

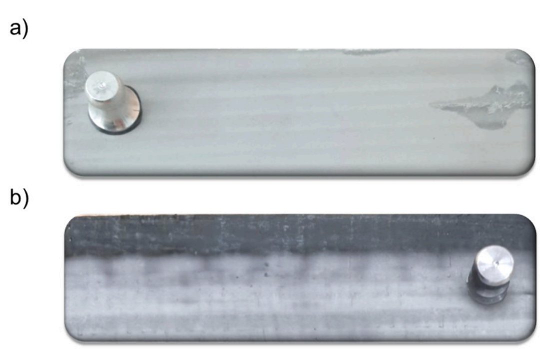

Fig. 5. Positioning of aluminum dolly for adhesion test on a) unreinforced substrate b) reinforced substrate.

for the pure polymeric substrates are reported in Table 3, in terms of difference between E_p (which is the amount of energy possessed by a single particle impacting the substrate) and E_a (which is the amount of energy required to activate the phenomena leading to the adhesion of the particle). It is worth to notice that the term accounting for the loading of the fibers has not been considered in this case.

It can be seen from Table 3 that when the particle impact velocity is low ($v_1 = 100$ m/s in this case), no deposition occurs, and the particles rebound from the substrate. By applying the *Vi-Pe-R-A* equation, the difference between the two members, e.g., E_p and E_a, respectively, is negative and equal to $\Delta E(v_1) = -1.9770 \cdot 10^{-6}$ J: the available energy is lower than the energy required to activate the phenomena supposed to be the ones ruling adhesion. That should mean the particle does not possess the right energy values to activate the adhesion mechanisms, as confirmed experimentally.

With the increase of the impact velocity ($v_2 = 225$ m/s in this case), the particles seem to adhere to the substrate; however, the relatively low values from adhesion tests confirm the poor deposition overall behavior observed, meaning that this velocity is not capable of ensuring a good anchoring of the particles with the substrate. The experimental evidence is reported in Fig. 7a. By applying the *Vi-Pe-R-A* equation, it results that E_p is slightly higher than E_a, as their difference $\Delta E(v_2) = 5.6932 \cdot 10^{-8}$ J is relatively low. Note that not all particles impact perfectly perpendicular to the substrate and that some dissipative causes (such as collisions between the particles that can slow down their path or other dissipative phenomena) were not considered by the model. That means $\Delta E(v_2)$ should be furtherly smaller, so resulting in very poor values of deposition efficiency and adhesion values.

If the particle impact velocity increases furtherly ($v_3 = 400$ m/s), an effective deposition of the particles was observed with the adhesion values equal to 6.4 MPa, in agreement with the literature [49]. In this case, an effective coverage was obtained, as confirmed by the picture shown in Fig. 7b. Under this condition, the model shows that E_p is noticeably higher than E_a, as proved by the difference $\Delta E(v_3) = 2.4015 \cdot 10^{-6}$ J. This means that the energy possessed by the particles is high enough to offset the dissipative phenomena occurring during the impact.

It is evident that the model proposed in the *Vi-Pe-R-A* equation is able to predict the experimental behavior of the particles during the deposition on a polymeric substrate with a reasonable level of accuracy.

As regards the reinforced specimens, the results given from the model that takes accounting also for the loading of the fibers, are reported in Table 4.

It can be seen from Table 4 that no deposition was obtained when the particle impact velocity is 225 m/s. In this case, in agreement with the experimental outcomes, the difference between E_p and E_a in the *Vi-Pe-R-A* equation is negative and equal to $\Delta E(v_1) = -1.3742 \cdot 10^{-6}$ J: the energy required for adhesion is greater than the energy possessed by the particle. In this case, contrary to what was observed for unreinforced polymeric substrates, the relatively higher value of impact velocity ($v_1 = 225$ m/s) is not so great enough to promote adhesion; this behavior is due to the presence of the fibers that modify the mechanical properties of the substrate [53].

By increasing the impact velocity ($v_2 = 400$ m/s), the particles seem to adhere to the reinforced substrate. Moreover, the results from the *Vi-Pe-R-A* equation showed that E_p is higher than E_a, as confirmed by the positive difference $\Delta E(v_2) = 1.5300 \cdot 10^{-6}$ J. However, a poor deposition was observed experimentally, as proved by the relatively low values from the adhesion tests. That means the impact velocity is not so great to ensure a good anchoring of the particle with the substrate. The reason is that the reinforcing fibers make the polymer stiffer and more resistant compared to unreinforced polymeric substrates and higher impact energies are required to activate the adhesion mechanism promoting the coating formation [54].

If the impact velocity increases and reaches 550 m/s, the deposition occurs as the particles achieved the right velocity to adhere with the

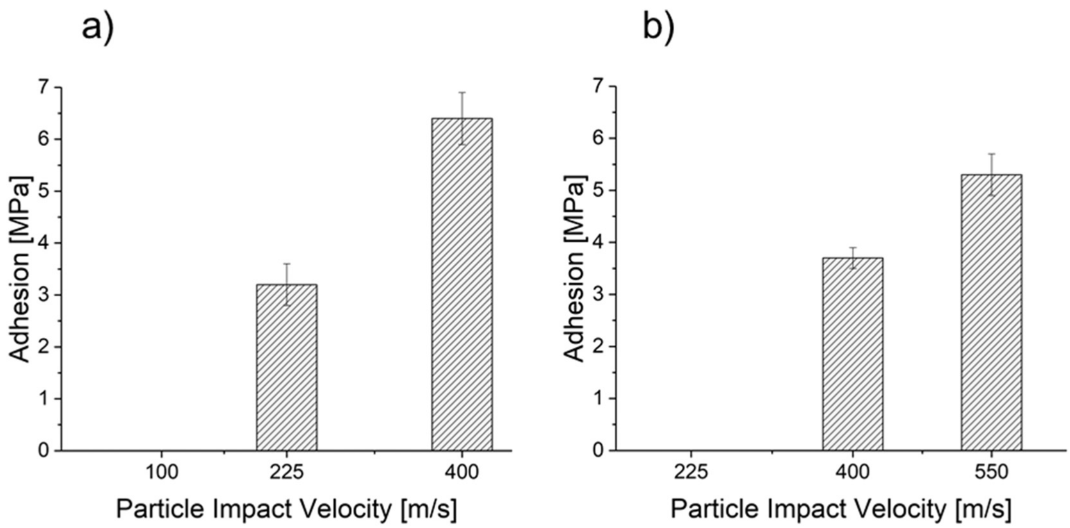

Fig. 6. Adhesion tests results for a) unreinforced substrates b) reinforced substrates.

Table 2
Main parameters required for the implementation of the model.

Material parameters for polymer	Polypropylene	
Melting temperature (T_f) [°C]	180	
Elastic modulus at 20 °C (E_s) [GPa]	1.63	
Yield strength at 20 °C (Y_s) [MPa]	30	
Thermal conductivity (K_m) [W/mK]	0.11	
Composite fiber main parameters	Carbon Fiber	
Elastic modulus (E_f) [GPa]	200	
Yield strength (Y_f) at 20 °C [MPa]	900	
Volume fraction in the composite [%]	50	
Thermal conductivity (K_f) [W/mK]	40	
Composite panel main characteristics	FRP	
Number of layers	15	
Matrix surface thickness [mm]	0.25	
Radius of the contact surface between the substrate and the particle (experimentally)	Polymer	FRP
a [mm]	0.025 ± 0.01	0.020 ± 0.01
Aluminum powder's main parameters		
Density, ρ_p [kg/m^3]	2700	–
Elastic modulus (E_{pow}) [GPa]	70	–
Yield strength (Y_p) at 20 °C [MPa]	290	–
Particle mass, m [Kg]	$3.8{\cdot}10^{-11}$	–
Particle mean radius, r [μm]	15	–
Particle semi-minor axis (after impact), r_1 [μm]	10	6
Thermal conductivity (K_p) [W/mK]	273	–

substrate. Also, the results from the model confirm this behavior, as proved by the greater positive difference between the two members of the *Vi-Pe-R-A* equation. However, under this condition, the experimental outcomes showed that degradation and erosion of the substrate took place due to the relatively high temperature values of the gas impinging onto the surface (as shown in Fig. 8). Note that this phenomenon was not taken into account by the *Vi-Pe-R-A* equation for which the substrate was considered at room temperature.

Based on these results, it is possible to assess that higher velocities are required to obtain adhesion on reinforced substrates, due to the higher properties of the composites, compared to pure polymeric substrates. However, due to the relatively high gas temperature involved to reach the right velocities, the polymeric material used to produce the composite should be carefully chosen aiming to prevent the erosion of the substrate during the deposition: high performance polymers (such as PEEK, for example) could represent a better choice to obtain good cold spray depositions.

Anyhow, in all the considered cases-study, the model seems to be able to predict the behavior of a particle during the impact, taking into account the presence of the fibers, hindering the penetration of the particle and the higher rigidity of the substrate. Therefore, based on these results, the model can be effectively applied to literature cases to assess its capability to describe the adhesion process.

4.2. Application of the model to literature cases

The model has been applied to three different cases, taken from literature, and the results are here reported. In choosing the cases it was decided to represent the following conditions: i) the deposition on a pure soft polymer; ii) the deposition on a pure high-performance polymer; iii) the deposition on a fiber-reinforced polymer. To this end, the comprehensive work of Che et al. [25] dealing with the deposition of copper on ABS and PEEK substrates under different processing conditions and the paper by Gillet et al. [31], dealing with the deposition on carbon fiber reinforced PEEK (CFRP), have been used. The depositions on pure ABS and PEEK substrates coated with copper powder were firstly considered under the two different impact velocities reported in literature: i) v_1 = 225 m/s; ii) v_2 = 500 m/s; the relative deposition efficiencies (*DE*) have been measured and reported by the authors [25]. The results given from model as well as the deposition efficiency measured are summarized in Table 5.

The first interesting result is that the model predicts lower energy required to achieve adhesion for ABS compared to the PEEK, which is coherent with the lower mechanical properties of ABS.

For the lower velocity (v_1 = 225 m/s), the energy possessed by the

Table 3
Experimental vs. theoretical results for cold spray deposition of aluminum particles on unreinforced polymeric substrates.

From Eq. (15)	From experimental tests		From *Vi-Pe-R-A* equation		
Particle impact velocity [m/s]	Overall behavior	Adhesion [MPa]	E_p [J]	E_a [J]	ΔE [J]
v_1 = 100	No deposition	n.a.	$4.5741{\cdot}10^{-7}$	$6.5511{\cdot}10^{-7}$	$-1.9770{\cdot}10^{-6}$
v_2 = 225	Poor deposition	3.2	$7.1200{\cdot}10^{-7}$	$6.5507{\cdot}10^{-7}$	$5.6932{\cdot}10^{-8}$
v_3 = 400	Effective deposition	6.4	$3.0564{\cdot}10^{-6}$	$6.5488{\cdot}10^{-7}$	$6.5893{\cdot}10^{-6}$

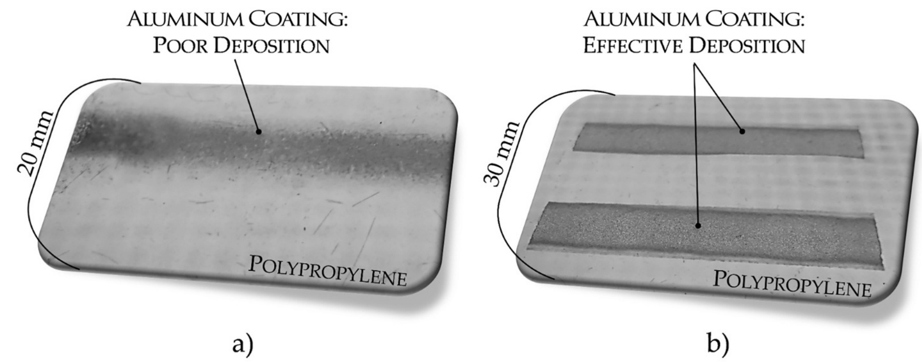

Fig. 7. Cold spray deposition of aluminum particles on unreinforced polymeric substrates varying the impact velocity: a) $v_2 = 225$ m/s (Poor deposition); b) $v_3 = 400$ m/s (effective deposition).

Table 4
Experimental vs. theoretical results for cold spray deposition of aluminum particles on fiber-reinforced polymer substrates.

From Eq. (15)	From experimental tests		From *Vi-Pe-R-A* equation		
Particle impact velocity [m/s]	Overall behavior	Adhesion [MPa]	E_p [J]	E_a [J]	ΔE [J]
$v_1 = 225$	No deposition	n.a.	$7.1200{\cdot}10^{-7}$	$2.0862{\cdot}10^{-6}$	$-1.3742{\cdot}10^{-6}$
$v_2 = 400$	Poor deposition	3.8	$3.0564{\cdot}10^{-6}$	$1.5263{\cdot}10^{-6}$	$1.5300{\cdot}10^{-6}$
$v_3 = 550$	Effective deposition with substrate erosion	5.3	$5.7765{\cdot}10^{-6}$	$1.5260{\cdot}10^{-6}$	$4.2501{\cdot}10^{-6}$

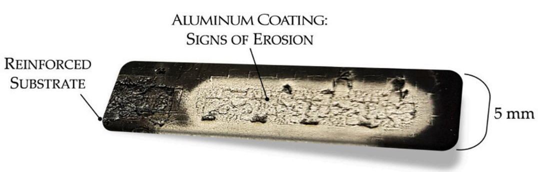

Fig. 8. Macrograph of CS deposition on fiber-reinforced composite substrates at $v_3 = 550$ m/s showing erosion of the substrate.

particle is higher than the one required for adhesion for both the substrates, as proved by the positive difference between E_p and E_a. However, it was observed an adequate deposition efficiency for ABS (>30 %) while a very poor one was observed for PEEK (<5 %). This experimental result can be better understood by looking at the outcomes from the model and considering that the available energy is in the proportion of about 20:1 with the energy required for adhesion for ABS, while it is about 10:1 for PEEK. Moreover, this is in agreement with the higher mechanical properties of PEEK, so more energy is required to activate the phenomena leading to adhesion.

For the higher velocity ($v_2 = 500$ m/s), the particle energy value exceeds two orders of magnitude the energy required for bonding with $\Delta E(v_2) = 1.5650{\cdot}10^{-5}$ J for ABS and $\Delta E(v_2) = 1.5605{\cdot}10^{-5}$ J for PEEK; in this case, completely different results were observed for the two materials. For PEEK, a good deposition was observed with a high deposition efficiency (>60 %), while severe erosion was observed for ABS. In this case, in contrast to what was found for PEEK, the energy possessed by the particles is too high at the impact with the ABS substrate (greater >80 times compared to the energy required for adhesion), which is characterized by relatively low mechanical properties and, therefore, it damages. Moreover, the deterioration of the polymer and the consequent erosion can be ascribed to the lower glass transition temperature of the ABS compared to the PEEK substrate, as the latter retains good mechanical properties at relatively high temperatures. Note that this was not taken into account by the model.

The *Vi-Pe-R-A* equation was also applied to study the deposition on a fiber-reinforced polymer. The work of Gillet et al. [31] studied the deposition of copper powders with different dimensions and the deposition efficiency versus the particle diameter was evaluated experimentally. The mean impact velocity for the three cases considered is 400 m/s. The particle mean diameters are: i) $d_1 = 10$ μm; ii) $d_2 = 23$ μm; iii) $d_3 = 38$ μm. The results given by the model as well as the deposition efficiency measured by the authors [31] are summarized in Table 6.

If the particles mean diameter is 10 μm, the energy required for the adhesion is moderately lower than the energy possessed by the particle. However, the available energy is greater >5 times compared to the energy required for bonding and the experimental analyses confirm the adhesion of the particles (DE = 28 %). This can be attributed to the higher deformation of the particles, which spread on the target surface promoted by the greater rigidity of the substrate. This result is very interesting in terms of the beneficial effects of the fibers reinforcing the polymeric substrate on CS deposition.

A small increase in the particle diameter produces an increase of both E_p and E_a values with the balance energy equal to $\Delta E(d_2) = 5.3612{\cdot}10^{-6}$ J. In this case, the available energy of the particle is in a proportion of 6:1 with the energy required for adhesion, which is about equal to the value reported for the previous condition ($d_1 = 10$ μm). However, the experimental results showed lower deposition efficiency values under

Table 5
Results from the literature cases: deposition of copper on ABS and PEEK substrates under different processing conditions.

Substrate	Particle impact velocity [m/s]	From literature		From *Vi-Pe-R-A* equation		
		Overall behavior	*DE* [%]	E_p [J]	E_a [J]	ΔE [J]
ABS	$v_1 = 225$	Effective deposition	30	$3.2089{\cdot}10^{-6}$	$1.8698{\cdot}10^{-7}$	$3.0219{\cdot}10^{-6}$
	$v_2 = 500$	Erosion	n.a.	$1.5837{\cdot}10^{-5}$	$1.8695{\cdot}10^{-7}$	$1.5650{\cdot}10^{-5}$
PEEK	$v_1 = 225$	Poor deposition	5	$3.2089{\cdot}10^{-6}$	$2.0229{\cdot}10^{-7}$	$2.9766{\cdot}10^{-6}$
	$v_2 = 500$	Effective deposition	60	$1.5837{\cdot}10^{-5}$	$2.0226{\cdot}10^{-7}$	$1.5605{\cdot}10^{-5}$

Table 6
Results from the literature cases: deposition of powders with different dimensions on a fiber-reinforced polymer.

Substrate	Particle mean diameter [μm]	From literature		From *Vi-Pe-R-A* equation		
		Overall behavior	*DE* [%]	E_p [J]	E_a [J]	ΔE [J]
CFRP	$d_1 = 10$	Effective deposition	28	$5.8655{\cdot}10^{-7}$	$9.9845{\cdot}10^{-8}$	$4.8671{\cdot}10^{-7}$
	$d_2 = 23$	Poor deposition	8.	$6.2456{\cdot}10^{-6}$	$8.8443{\cdot}10^{-7}$	$5.3612{\cdot}10^{-6}$
	$d_3 = 38$	Fiber damage	<5	$2.7366{\cdot}10^{-5}$	$3.8911{\cdot}10^{-6}$	$2.3475{\cdot}10^{-5}$

these conditions, with the particles exhibiting less deformation as well as higher penetration when impacting the composite substrate. This experimental-observed condition is related to the damage of the fibers that was not taken into account by the model.

For the biggest diameter ($d_3 = 38$ μm), it can be seen again that the available energy is >6 times compared to the energy required for adhesion, meaning that an effective deposition can occur, as shown for the first case ($d_1 = 10$ μm). However, under this condition, the damage of the fibers was found experimentally with the coating that is carried away by the impinging particles that possess a high amount of kinetic energy.

5. Discussion

5.1. Adhesion mechanism

The first point interesting to discuss is that the model seems to well describe the literature experimental outcomes, the observed results in terms of deposition efficiency can be explained on the basis of the difference between the E_p and E_a, as defined by the model. When ΔE was relatively low, the experiments in the literature showed a very low value of the deposition efficiency; it can be argued that in this case, only the particles with an impact angle close to 90° have enough energy to activate the conjectured phenomena, leading to the low value observed of the deposition efficiency. This can be asserted because the model does not consider some dissipative events like impacts among the particles and angles of impact different from 90°, so it can be assumed that the effective E_p was lower than E_a and then there is not enough energy to achieve adhesion. An increase of the deposition efficiency was observed when ΔE increases until this difference becomes too high and the erosion of the substrate is observed. This suggests that for a higher value of E_p the particle has energy enough to activate phenomena such as damage of the fibers, breaking of the polymer that leads to global erosion behavior. Different results, in terms of ΔE thresholds, were obtained for reinforced polymers and simple polymers, these results highlighted the role paid by the fibers and corroborated the choice to introduce fibers related terms in our model. It seems that the presence of the fibers strengthens the substrate causing the particles plastically deform more. Such a result is also well described by the model (cfr. *A* and *B* coefficients).

Considering the results, it is possible to suggest that the prevailing mechanism is the mechanical interlocking between the particle and the substrate: no chemical reaction between the powder and the substrate occurs and, as confirmed by previous literature works [47], the thermal softening is not necessary for the onset of jetting. This phenomenon occurs mainly due to the plastic deformation of the substrate. If the substrate is stiff enough, and the powder is a soft metal, plastic deformation of the particle can be also expected. When both the substrate and the particle contribute to the plastic deformation, a better deposition efficiency is observed.

It is also interesting to discuss the contribution of the conjectured phenomena under the light of the energy required which is portrayed in Table 7.

Observing the values of the different contributions presented in Table 7, it is evident that the presence of the fibers strongly influences the deposition. In fact, due to the fibers stiffening effect, the reinforced substrate requires more energy to be deformed of the same quantity (as evidenced by comparing the values of the energy required to plastically

Table 7
Single energy contribution to particle adhesion for an aluminum particle on composite and pure polymeric substrate ($v = 400$ m/s), where $E_{PLA(s)}$ and $E_{PLA(p)}$ are the energy values required to plastically deform the substrate and the particle, respectively; E_{load} is the energy required for the loading of the fibers and E_T is the thermal energy.

	$E_{PLA(s)}$ [J]	$E_{PLA(p)}$ [J]	E_{load} [J]	E_T [J]
FRP	$3.40{\cdot}10^{-6}$	$9.22{\cdot}10^{-7}$	$1.24{\cdot}10^{-5}$	$1.70{\cdot}10^{-10}$
Pure Polymer	$4.62{\cdot}10^{-8}$	$4.07{\cdot}10^{-7}$	0	$1.70{\cdot}10^{-10}$

deform the substrate for the composite substrate and the pure polymeric substrate, $E_{PLA(s)}$). It is possible to assess that the substrate characteristics have a crucial role in the deposition and have to be carefully considered. The role of the fibers in the deposition will be furtherly investigated in the next paragraph.

5.2. Role of the fibers

The fibers have a complex influence on the adhesion: on one hand, the particle energy is partially absorbed by the loading of the fibers, on the other hand, the presence of the fibers promotes the deformation of the particle by strengthening the matrix. Plus, the physical presence of the fibers limits the plunging depth that the particle can achieve because at a certain point the particle touches and damages the fiber. Both these evidences can be explained by considering the sketch reported in Fig. 9.

The first row is representative of the low velocity impact. In the case of pure polymer, the particle impacts on a relatively soft material characterized by a reduced stiffness; the result is that the particle does not experience plastic deformation, so the surplus of energy is used to produce the rebounding phenomenon, hampering the adhesion. On the other hand, as shown in the second raw of Fig. 9a, when the surplus of energy becomes very high, the particle can penetrate the polymeric matrix that plastically deforms and tends to embed the particle, so promoting the interlocking mechanism. In FRPs, the fibers reinforcement stiffens the polymeric substrate and promotes the particle deformation and adhesion, as shown in Fig. 9b (top). However, with the increasing of the impact velocity, the particle could have enough energy to penetrate within the matrix, impacting with the fibers reinforcement that can fail and break, as schematically shown in Fig. 9b (bottom). Moreover, as confirmed by literature [31,55], the influence of the fibers and the consequent lowering of the deposition window is strongly dependent on the surface matrix thickness of the fiber-reinforced substrate. In fact, as a thicker layer of polymer is present on the surface, the impact behavior of the composite tends to draw nearer to the pure polymeric substrate behavior. Therefore, the composite substrate needs to be accurately designed in order to guarantee the best performances when spraying metal powders. This crucial aspect should be carefully considered in further developments of this model.

5.3. Predictive simulations through Vi-Pe-R-A equation

The *Vi-Pe-R-A* equation can be used as a valid tool to perform qualitative analyses to predict the outcomes of the process, varying the feedstock properties and process conditions of cold spray depositions on polymer-based materials. In this section, the influence of some peculiar parameters on CS deposition will be assessed, and the *Vi-Pe-Ra* equation

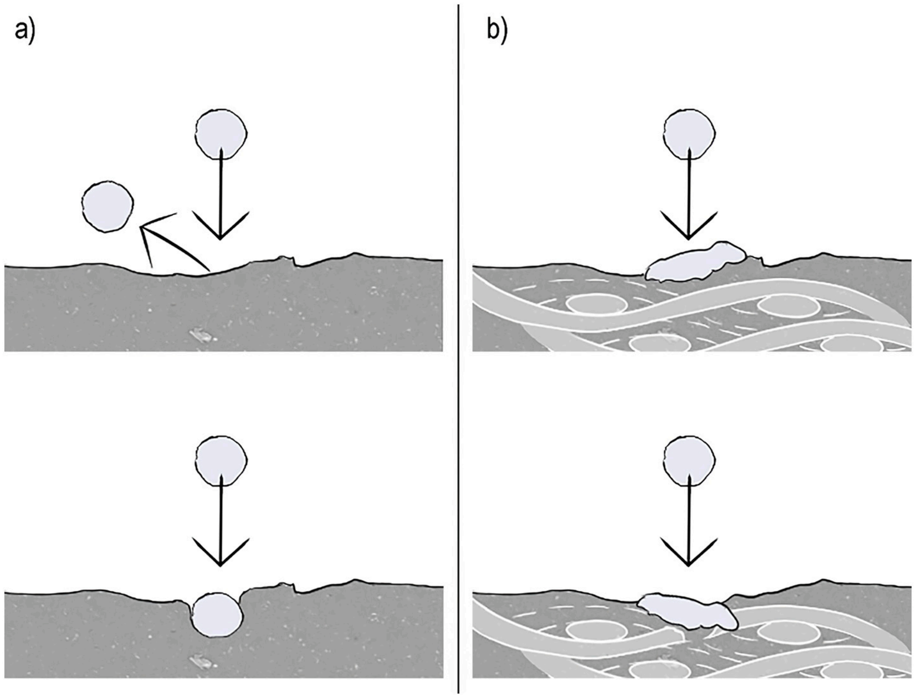

Fig. 9. Sketches of the impacts for increasing ΔE values (a given ΔE for each raw in the figure) with different substrates: a) impact of a particle on a pure polymeric substrate, b) impact of a particle on a composite substrate.

will be employed aiming to provide further insights into the cold spray process.

The parameters influencing the deposition of metallic particles on polymer-based substrates were classified here into three main categories, for the clarity of the discussion: the powder parameters, the process parameters and the substrates parameters. A single parameter was chosen for each category and its effect on CS deposition was analyzed. In particular, the influence of i) the particle size, ii) the particle impact velocity and iii) the fiber volume percentage within the composite substrate was examined through the *Vi-Pe-R-A* equation.

5.3.1. Influence of the particle size

Aiming to assess the influence of the particle size when cold spraying on polymers, the energy possessed by the particle and the energy required to obtain adhesion (namely E_p and E_a, respectively) have been plotted with respect to the mean radius of the powders, keeping constant all the remaining parameters that do not involve the particle radius in the *Vi-Pe-R-A* equation. In agreement with the materials used for the experimental validation of the theoretical model (more details in Section 3), a sheet of polypropylene was considered as substrate and AlSi10Mg aluminum powders were chosen as impacting particles.

For this scope, three different values of impact velocity were considered, chosen accordingly to the experiments presented in the previous section: $v_1 = 100$ m/s, $v_2 = 225$ m/s and $v_3 = 400$ m/s. The predictive results obtained are shown in Fig. 10. It is worth noticing that E_a is scarcely influenced by the impact velocity, as expected through the *Vi-Pe-R-A* equation. In fact, the curves obtained for the three values of impact velocity appear to overlap in the figure. This is furtherly highlighted by observing the magnification in Fig. 10. It is possible to note that by increasing the particle size, the energy possessed by the particle increases. However, regardless of the particle radius chosen, when the particles are sprayed with the lowest impact velocity (v_1), the adhesion never occurs, as confirmed by experimental data obtained for the 30 μm diameter.

On the other hand, for higher impact velocities (v_2 and v_3) the adhesion occurs for every value of the radius of the powder considered. It is crucial to observe that for relatively small diameter values, the energy surplus possessed by the particle could not be great enough to obtain good adhesion as some dissipative phenomena have not been considered within the model. In fact, for very small values of the particle radius (lower than 15 μm), the E_p and E_a curves tend to overlap. For this reason, spraying relatively bigger particles could lead to better-adhered coatings regardless of impact velocity.

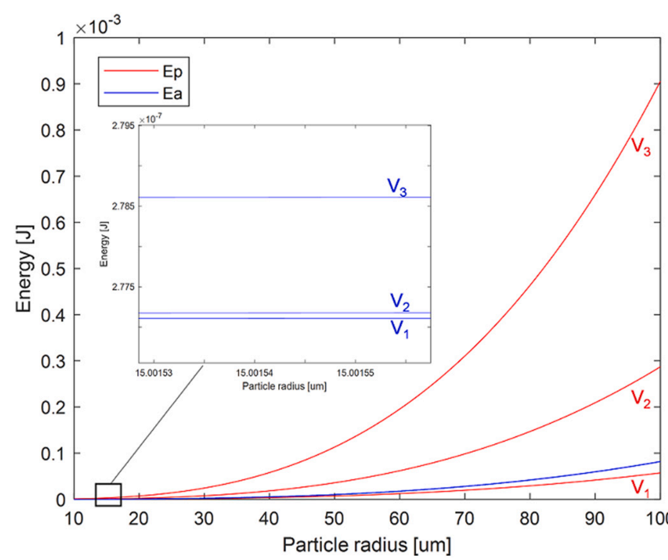

Fig. 10. Predictive simulations through *Vi-Pe-R-A* equation showing the trend of E_p and E_a with the particle size for three different impact velocities: $v_1 = 100$ m/s, $v_2 = 225$ m/s and $v_3 = 400$ m/s.

5.3.2. Influence of the particle impact velocity

The particle impact velocity is the most important cold spray process parameter that influences the bonding phenomena. It is the result of the process parameters chosen for the deposition, such as the gas temperature, the gas pressure and the stand-off distance, which have to be properly set for the coating formation and grow-up.

Both the E_p and E_a energy curves were plotted by varying the particle impact velocity for three different powder materials (Fig. 11). In particular, the *Vi-Pe-R-A* equation was particularized for aluminum, steel and copper materials in order to assess the capability of the model to predict the behavior of a wide range of materials characterized by different densities and mechanical characteristics. The particle diameter was kept equal to 30 μm. The unreinforced polypropylene (whose characteristics are reported in Section 3) was chosen for this analysis.

The model was proved to be able of predicting the critical velocity, v_{crit} (namely, the threshold velocity above which the adhesion occurs) for all the powder materials considered, as evident in Fig. 11. In fact, the critical velocity can be found at the intersection point between E_p and E_a curves, as it is the minimum value of velocity required to obtain adhesion.

The steel and copper curves showing the energy possessed by the particle (E_p in Fig. 11b and c) are characterized by a greater slope compared to aluminum (Fig. 11a): in fact, those particles possess higher energy when sprayed with the same process parameters due to the relatively greater mass density. However, the mechanical properties of aluminum are lower than those of steel; in particular, the particle made of aluminum is characterized by a lower yield strength (290 MPa), so resulting in a more ductile and deformable material when sprayed onto the substrate. The result is that it is easier to deposit aluminum particles compared to steel, characterized by a yield strength of 350 MPa.

It is also possible to observe from Fig. 11c that copper, which is the material characterized by the lowest value of yield strength (33 MPa) and highest value of density among the three materials under examination, has the lowest value of critical velocity (52 m/s), resulting to be the easiest material to deposit compared to steel and aluminum.

It is known from literature that when cold spraying on metallic substrates, it is possible to define an erosion velocity as the upper limit of the particle impact velocity above which the erosive effects, due to hydrodynamic penetration of the substrate by the particles, occur. This phenomenon is known from large-scale impact dynamics and can also be applied to cold spray [56]. When cold spraying on polymers, it is crucial to underline that the concept of erosion of a polymeric substrate impacted by metal particles is not clearly defined in the literature. In fact, the phenomena occurring when the particles impact the substrate with a velocity higher than the critical one without obtaining adhesion, are yet to be understood. For this reason, in this work, the erosion velocity has been assessed experimentally for a single case study, as the *Vi-Pe-R-A* equation does not take into account these phenomena. The deposition window for the aluminum case study is shown in Fig. 12.

It can be noticed that the critical velocity (120 m/s) was determined at the intersection point between E_p and E_a curves, while the erosion velocity (for the PP substrate) was found from experimental tests to be equal to 600 m/s.

5.3.3. *Influence of the fiber volume percentage within the composite substrate*

The *Vi-Pe-R-A* equation can represent an effective tool to evaluate the effects of the fiber volume percentage within the composite substrate on CS deposition. In this section, AlSi10Mg aluminum powders (30 μm as mean diameter) were chosen as impacting particles and sheets of polypropylene reinforced with carbon fibers were considered as substrates for the analyses. Both the E_p and E_a energy curves were plotted by varying the fiber volume percentage for two different impact velocities, v_1 = 225 m/s and v_2 = 304 m/s; the results are shown in Fig. 13.

It can be seen from the figure that the energy required for adhesion (E_a) tends to increase with the increase of the fiber volume percentage due to the stiffening effects of the fibers. If the particle impact velocity is set to 225 m/s and the composite substrate is characterized by a fiber volume percentage equal to 50 % (which are the conditions tested experimentally), the particles cannot adhere to the target surface, as the energy required for adhesion is greater than the energy possessed by the particle. This is the reason for which no bonding was observed experimentally under these conditions (see Table 4 for details). However, observing the figure, it is possible to assess that there is an upper limit of fiber volume percentage above which the considered impact velocity

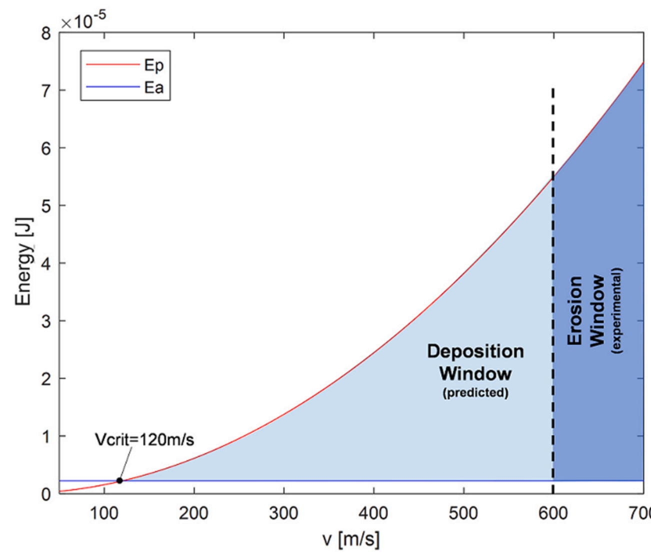

Fig. 12. Deposition window when cold spraying aluminum particles (30 μm) on PP substrate.

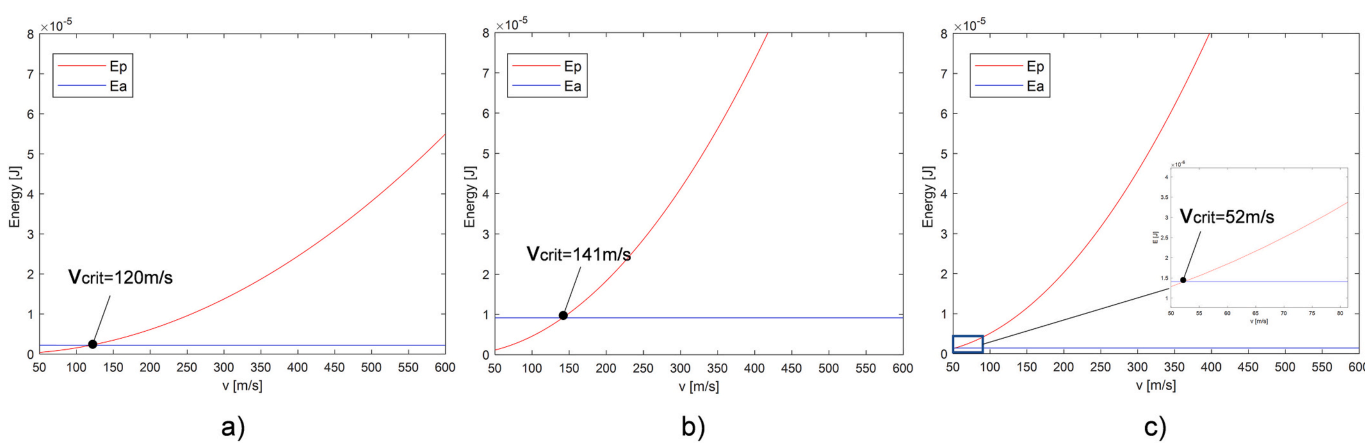

Fig. 11. Plot of E_p and E_a by varying the particle impact velocity for three different powder materials: a) aluminum b) steel c) copper.

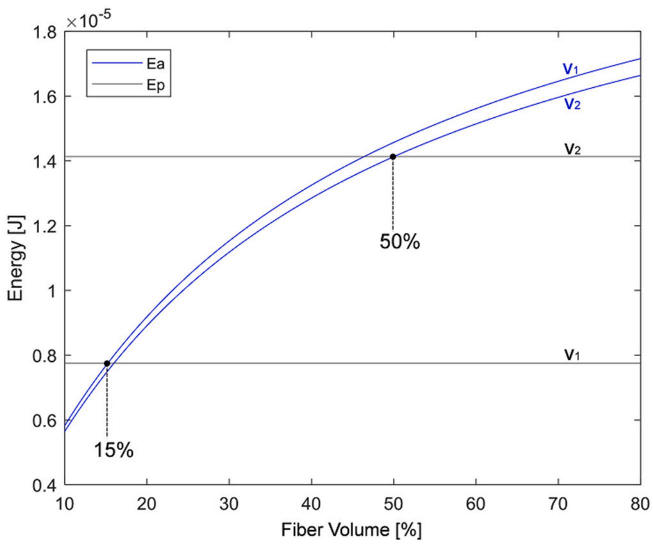

Fig. 13. Plot of E_p and E_a by varying the fiber volume percentage for two different impact velocities, $v_1 = 225$ m/s and $v_2 = 304$ m/s. Aluminum particles on reinforced PP substrate.

would not be sufficient to obtain adhesion. In this case, for a composite characterized by a fiber volume percentage lower than 15 %, the adhesion could occur as the substrate would be less stiff and would easily deform for the anchorage of the particle. The minimum particle velocity required for adhesion when the polymeric PP substrate is reinforced with a carbon fiber volume percentage of 50 % (which are the tested conditions reported in Table 4) is 304 m/s, as also shown in Fig. 13. That means that if the aluminum particle is sprayed with those parameters, it would be possible to obtain the deposition on a composite substrate with a fiber volume percentage equal or lower than 50 %.

The model could also be useful to properly assess the best lay-up strategy of the substrate and predict the best process parameters to employ to spray on composite characterized by different volume percentages.

6. Conclusions

Based on the results presented and discussed in the previous sections, it can be asserted that in this work, for the first time in literature, a theoretical model was proposed to clarify which are the phenomena occurring as a result of the impact of a particle on a polymer matrix composite substrate that leads to the coating formation in cold spraying. The model proved to be a helpful tool to predict the bonding conditions for different powder/substrate material configurations, so providing the proper CS process parameters to be set for deposition. The *Vi-Pe-R-A* equation shows promises of being a useful tool to expand the industrial applications of cold spray technology.

The detailed results of this work can be summarized as follows:

- The proposed model can predict if adhesion will occur, the validation was successfully carried out by designing a dedicated experimental campaign whose results showed that the ΔE, as defined by using the *Vi-Pe-R-A* equation, is a reliable parameter to predict the adhesion.
- It was assessed that the model well describes the physics of the process; with the increasing of the ΔE a transition from rebound to adhesion to erosion is observed; ΔE can be adopted as a criterion to predict if adhesion will occur, of course the threshold values need to be carefully found for each combination of powder/substrate.
- Relying on the proposed model it can be said that the main phenomena ruling the adhesion of metallic particles on polymeric substrates are: dissipation, plastic deformation of the substrate, plastic deformation of the particle and fiber loading. The prevailing mechanism, and the most energy-demanding, is the plastic deformation of the substrate. The distribution of the available energy among the different phenomena is influenced by the mechanical properties of the powder and of the substrate; regarding composite substrates the presence of the fibers contributes to hinder the deformation of the substrate and increases the deformation of the impacting powders by stiffening the substrate itself.
- The adhesion occurs due to the mechanical interlock between the particles and the substrate, this mechanical interlock is produced thanks to the mutual plastic deformation of both particles and substrate.
- The model, applied to literature cases, was proved to be able to describe properly the experimental outcomes observed, moreover it allowed to better understand the reported results.
- The model can be used to choose the particle velocity to reach, once the properties of substrate and particles are well known.
- The substrate has a fundamental role in the process, the presence of the fibers and the stratification sequence strongly change the adhesion conditions, as a consequence the design of the panel is part of the processing conditions to be set.

In summary, when cold spraying metal onto polymers, relatively big particles are recommended (>30 μm) to obtain better-adhered coatings regardless of impact velocity. The copper particles can be easily deposited onto soft polymers, like PP, by setting an impact velocity higher than 52 m/s, while the deposition of aluminum particles and, even more, that of steel particles, is more difficult as higher impact velocities must be reached (>120 m/s for aluminum and >141 m/s for steel). If the polymer is fiber-reinforced, the velocity required for adhesion increases; in particular, an impact velocity higher than 304 m/s must be set for the aluminum particles when the polymeric PP substrate is reinforced with a carbon fiber volume percentage of 50 %.

CRediT authorship contribution statement

Alessia Serena Perna: Conceptualization, Methodology, Software, Validation, Formal analysis, Writing - Original Draft; **Antonio Viscusi:** Conceptualization, Methodology, Validation, Formal analysis, Writing - Review & Editing; **Roberta Della Gatta:** Investigation, Data Curation; **Antonello Astarita:** Conceptualization, Supervision, Visualization, Project administration.

Declaration of competing interest

The authors declare that they have no conflict of interest.

Data availability

Data will be made available on request.

Acknowledgements

The authors want to warmly thank Professor Luigi Carrino for constantly guiding and inspiring our work, creating the conditions for us to carry on this project and for his precious scientific advices.

References

[1] A. Papyrin, The development of the cold spray process, in: The Cold Spray Materials Deposition Process: Fundamentals and Applications, 2007, pp. 11–42, https://doi.org/10.1533/9781845693787.1.11.
[2] M. Jeandin, F. Delloro, P.E. Léger, V. Bortolussi, M. Sennour, Cold spray under the banner of thermal spray in the whirlwind of additive manufacturing, Surf. Eng. (2018) 1–6, https://doi.org/10.1080/02670844.2018.1471188.
[3] T. Schmidt, F. Gärtner, H. Assadi, H. Kreye, Development of a generalized parameter window for cold spray deposition, Acta Mater. 54 (2006) 729–742, https://doi.org/10.1016/j.actamat.2005.10.005.

[4] T. Schmidt, H. Assadi, F. Gärtner, H. Richter, T. Stoltenhoff, H. Kreye, T. Klassen, From particle acceleration to impact and bonding in cold spraying, J. Therm. Spray Technol. 18 (2009) 794–808, https://doi.org/10.1007/s11666-009-9357-7.
[5] H. Assadi, H. Kreye, F. Gärtner, T. Klassen, Cold spraying – a materials perspective, Acta Mater. 116 (2016) 382–407, https://doi.org/10.1016/j.actamat.2016.06.034.
[6] A. Papyrin, V. Kosarev, S. Klinkov, A. Alkimov, V. Fomin, Discovery of the cold spray phenomenon and its basic features, Cold SprayTechnol. (2007) 1–32, https://doi.org/10.1016/b978-008045155-8/50001-6.
[7] H. Assadi, F. Gärtner, T. Stoltenhoff, H. Kreye, Bonding mechanism in cold gas spraying, Acta Mater. 51 (2003) 4379–4394, https://doi.org/10.1016/S1359-6454(03)00274-X.
[8] K.H. Ko, J.O. Choi, H. Lee, The interfacial restructuring to amorphous: a new adhesion mechanism of cold-sprayed coatings, Mater. Lett. 175 (2016) 13–15, https://doi.org/10.1016/j.matlet.2016.03.132.
[9] X.T. Luo, C.X. Li, F.L. Shang, G.J. Yang, Y.Y. Wang, C.J. Li, High velocity impact induced microstructure evolution during deposition of cold spray coatings: a review, Surf. Coat. Technol. 254 (2014) 11–20, https://doi.org/10.1016/j.surfcoat.2014.06.006.
[10] V.K. Champagne, M.K. West, M. Reza Rokni, T. Curtis, V. Champagne, B. McNally, Joining of cast ZE41A mg to wrought 6061 Al by the cold spray process and friction stir welding, J. Therm. Spray Technol. 25 (2016) 143–159, https://doi.org/10.1007/s11666-015-0301-8.
[11] M. Hassani-Gangaraj, D. Veysset, V.K. Champagne, K.A. Nelson, C.A. Schuh, Adiabatic shear instability is not necessary for adhesion in cold spray, Acta Mater. 158 (2018) 430–439, https://doi.org/10.1016/j.actamat.2018.07.065.
[12] G. Bae, J. Il Jang, C. Lee, Correlation of particle impact conditions with bonding, nanocrystal formation and mechanical properties in kinetic sprayed nickel, Acta Mater. 60 (2012) 3524–3535, https://doi.org/10.1016/j.actamat.2012.03.001.
[13] M. Grujicic, C.L. Zhao, W.S. DeRosset, D. Helfritch, Adiabatic shear instability based mechanism for particles/substrate bonding in the cold-gas dynamic-spray process, Mater. Des. 25 (2004) 681–688, https://doi.org/10.1016/j.matdes.2004.03.008.
[14] V.K. Champagne, V.K. Champagne, The cold spray materials deposition process, Fundam. Appl. 2007 (2007).
[15] M. Gardon, A. Latorre, M. Torrell, S. Dosta, J. Fernández, J.M. Guilemany, Cold gas spray titanium coatings onto a biocompatible polymer, Mater. Lett. 106 (2013) 97–99, https://doi.org/10.1016/J.MATLET.2013.04.115.
[16] M.J. Vucko, P.C. King, A.J. Poole, C. Carl, M.Z. Jahedi, R. de Nys, Cold spray metal embedment: an innovative antifouling technology, Biofouling 28 (2012) 239–248, https://doi.org/10.1080/08927014.2012.670849.
[17] A. Małachowska, L. Pawłowski, M. Winnicki, T. Piasecki, A. Ambroziak, in: The Possibility of Cold Spray Process Application to Obtain Electrically Conductive Coatings on Polymers, ITCS 2015 - Proceedings of the International Thermal Spray Conference, 2015, pp. 1159–1164, https://doi.org/10.13140/RG.2.1.3267.9848.
[18] J. Affi, H. Okazaki, M. Yamada, M. Fukumoto, Fabrication of aluminum coating onto CFRP substrate by cold spray, Mater. Trans. 52 (2011) 1759–1763, https://doi.org/10.2320/matertrans.T-M2011807.
[19] R.N. Raoelison, C. Verdy, H. Liao, Cold gas dynamic spray additive manufacturing today: deposit possibilities, technological solutions and viable applications, Mater. Des. (2017), https://doi.org/10.1016/j.matdes.2017.07.067.
[20] R. Lupoi, W. O'Neill, Deposition of metallic coatings on polymer surfaces using cold spray, Surf. Coat. Technol. 205 (2010) 2167–2173, https://doi.org/10.1016/j.surfcoat.2010.08.128.
[21] X.L. Zhou, A.F. Chen, J.C. Liu, X.K. Wu, J.S. Zhang, Preparation of metallic coatings on polymer matrix composites by cold spray, Surf. Coat. Technol. 206 (2011) 132–136, https://doi.org/10.1016/j.surfcoat.2011.07.005.
[22] J. Affi, H. Okazaki, M. Yamada, M. Fukumoto, Fabrication of aluminum coating onto CFRP substrate by cold spray, Mater. Trans. 52 (2011) 1759–1763, https://doi.org/10.2320/matertrans.T-M2011807.
[23] H. Che, P. Vo, S. Yue, Metallization of carbon fibre reinforced polymers by cold spray, Surf. Coat. Technol. 313 (2017) 236–247, https://doi.org/10.1016/j.surfcoat.2017.01.083.
[24] H. Che, P. Vo, S. Yue, Investigation of cold spray on polymers by single particle impact experiments, J. Therm. Spray Technol. 28 (2019) 135–143, https://doi.org/10.1007/s11666-018-0801-4.
[25] H. Che, X. Chu, P. Vo, S. Yue, Metallization of various polymers by cold spray, J. Therm. Spray Technol. 27 (2018) 169–178, https://doi.org/10.1007/s11666-017-0663-1.
[26] H. Che, X. Chu, P. Vo, S. Yue, Cold spray of mixed metal powders on carbon fibre reinforced polymers, Surf. Coat. Technol. 329 (2017) 232–243, https://doi.org/10.1016/j.surfcoat.2017.09.052.
[27] A. Astarita, L. Boccarusso, M. Durante, A. Viscusi, R. Sansone, L. Carrino, Study of the production of a metallic coating on natural fiber composite through the cold spray technique, J. Mater. Eng. Perform. 27 (2018) 739–750, https://doi.org/10.1007/s11665-018-3147-7.
[28] L. Boccarusso, A. Viscusi, M. Durante, A. Astarita, D. De Fazio, R. Sansone, A. Caraviello, L. Carrino, Deposition of aluminum coatings on bio-composite laminates, in: AIP Conference Proceedings 1960, 2018, https://doi.org/10.1063/1.5034944.
[29] A.S. Perna, A. Viscusi, A. Astarita, L. Boccarusso, L. Carrino, M. Durante, R. Sansone, Manufacturing of a metal matrix composite coating on a polymer matrix composite through cold gas dynamic spray technique, J. Mater. Eng. Perform. 28 (2019) 3211–3219, https://doi.org/10.1007/s11665-019-03914-6.
[30] A. Ganesan, M. Yamada, M. Fukumoto, Cold spray coating deposition mechanism on the thermoplastic and thermosetting polymer substrates, J. Therm. Spray Technol. 22 (2013) 1275–1282, https://doi.org/10.1007/s11666-013-9984-x.
[31] V. Gillet, E. Aubignat, S. Costil, B. Courant, C. Langlade, P. Casari, W. Knapp, M. P. Planche, Development of low pressure cold sprayed copper coatings on carbon fiber reinforced polymer (CFRP), Surf. Coat. Technol. 364 (2019) 306–316, https://doi.org/10.1016/j.surfcoat.2019.01.011.
[32] A. Viscusi, V. Antonucci, L. Carrino, R. Della Gatta, V. Lopresto, I. Papa, A.S. Perna, M.R. Ricciardi, A. Astarita, Manufacturing of an innovative composite structure: design, manufacturing and impact behaviour, Compos. Struct. 250 (2020), https://doi.org/10.1016/j.compstruct.2020.112637.
[33] Y. Xiong, G. Bae, X. Xiong, C. Lee, The effects of successive impacts and cold welds on the deposition onset of cold spray coatings, J. Therm. Spray Technol. (2010), https://doi.org/10.1007/s11666-009-9455-6.
[34] T.W. Leland, G.a Mansoori, in: Basic Principles of Classical and Statistical Thermodynamics, 1986, pp. 1–35.
[35] M. Faizan-Ur-Rab, S.H. Zahiri, S.H. Masood, T.D. Phan, M. Jahedi, R. Nagarajah, Application of a holistic 3D model to estimate state of cold spray titanium particles, Mater. Des. 89 (2016) 1227–1241, https://doi.org/10.1016/j.matdes.2015.10.075.
[36] K.L. Johnson, Contact Mechanics, Cambridge University Press, Cambridge, 1985, https://doi.org/10.1017/CBO9781139171731.
[37] R.L. Jackson, I. Green, D.B. Marghitu, Predicting the coefficient of restitution of impacting elastic-perfectly plastic spheres, Nonlinear Dyn. 60 (2010) 217–229, https://doi.org/10.1007/s11071-009-9591-z.
[38] G.E. Dieter, D. Bacon, Mechanical Metallurgy, McGraw-Hill, 1988. https://books.google.it/books?id=hlabmB3e8XwC.
[39] S.S. Morye, P.J. Hine, R.A. Duckett, D.J. Carr, I.M. Ward, Modelling of the energy absorption by polymer composites upon ballistic impact, Compos. Sci. Technol. 60 (2000) 2631–2642, https://doi.org/10.1016/S0266-3538(00)00139-1.
[40] R. Della Gatta, A. Viscusi, A.S. Perna, A. Caraviello, A. Astarita, Feasibility of steel powder deposition on composites through cold spray, Mater. Manuf. Process. 36 (2021) 281–291, https://doi.org/10.1080/10426914.2020.1832693.
[41] M.R. Rokni, P. Feng, C.A. Widener, S.R. Nutt, Depositing Al-based metallic coatings onto polymer substrates by cold spray, J. Therm. Spray Technol. 28 (2019) 1699–1708, https://doi.org/10.1007/s11666-019-00911-y.
[42] A. Viscusi, A.S. Perna, A. Caraviello, A. Astarita, R. della Gatta, Cold spray process for the production of AlSi10Mg coatings on glass fibers reinforced polymers, Materials and Manufacturing Processes. 36 (2021), https://doi.org/10.1080/10426914.2020.1813895.
[43] A. Viscusi, A.S. Perna, A. Astarita, L. Boccarusso, A. Caraviello, L. Carrino, R. D. Gatta, M. Durante, R. Sansone, Experimental Study of Cold Sprayed Metallic Coatings on Thermoplastic Matrix Composites, 2019, https://doi.org/10.4028/www.scientific.net/KEM.813.68.
[44] I. Papa, P. Russo, A. Astarita, A. Viscusi, A.S. Perna, L. Carrino, V. Lopresto, Impact behaviour of a novel composite structure made of a polymer reinforced composite with a 3D printed metallic coating, Compos. Struct. 245 (2020), https://doi.org/10.1016/j.compstruct.2020.112346.
[45] D.L. Gilmore, R.C. Dykhuizen, R.A. Neiser, M.F. Smith, T.J. Roemer, Particle velocity and deposition efficiency in the cold spray process, J. Therm. Spray Technol. 8 (1999) 576–582, https://doi.org/10.1361/105996399770350278.
[46] S. Yavuzkurt, A guide to uncertainty analysis of hot-wire data, J. Fluids Eng. 106 (1984) 181–186, https://doi.org/10.1115/1.3243096.
[47] A.P. Alkhimov, V.F. Kosarev, S.v. Klinkov, The features of cold spray nozzle design, Journal of Thermal Spray Technology. 10 (2001) 375–381, https://doi.org/10.1361/105996301770349466.
[48] J. Wu, H. Fang, S. Yoon, H. Kim, C. Lee, Measurement of particle velocity and characterization of deposition in aluminum alloy kinetic spraying process, Appl. Surf. Sci. 252 (2005) 1368–1377, https://doi.org/10.1016/j.apsusc.2005.02.108.
[49] A.S. Perna, A. Viscusi, R. della Gatta, A. Astarita, Integrating 3D printing of polymer matrix composites and metal additive layer manufacturing: surface metallization of 3D printed composite panels through cold spray deposition of aluminium particles, International Journal of Material Forming. 15 (2022) 15, https://doi.org/10.1007/S12289-022-01665-9.
[50] H. Che, P. Vo, S. Yue, Investigation of cold spray on polymers by single particle impact experiments, J. Therm. Spray Technol. 28 (2019) 135–143, https://doi.org/10.1007/s11666-018-0801-4.
[51] M. Faizan-Ur-Rab, S.H. Zahiri, S.H. Masood, T.D. Phan, M. Jahedi, R. Nagarajah, Application of a holistic 3D model to estimate state of cold spray titanium particles, Mater. Des. 89 (2016) 1227–1241, https://doi.org/10.1016/j.matdes.2015.10.075.
[52] H. Katanoda, M. Fukuhara, N. Iino, Numerical study of combination parameters for particle impact velocity and temperature in cold spray, J. Therm. Spray Technol. 16 (2007) 627–633, https://doi.org/10.1007/s11666-007-9087-7.
[53] A. Viscusi, M. Durante, A. Astarita, L. Boccarusso, L. Carrino, A.S. Perna, Experimental evaluation of metallic coating on polymer by cold spray, Procedia Manuf. (2020), https://doi.org/10.1016/j.promfg.2020.04.232.
[54] A.S. Perna, A. Viscusi, G. Pasquino, A. Astarita, Cold spray deposition of metallic coatings on polymers: a review, Journal of Materials Science (2021), https://doi.org/10.1007/s10853-021-06561-2.
[55] I. Papa, P. Russo, A. Astarita, A. Viscusi, A.S. Perna, L. Carrino, V. Lopresto, Influence of the metallic cold spray deposition on the low-velocity impact behaviour of composite laminates, Key Eng. Mater. (2019) 376–380, https://doi.org/10.4028/www.scientific.net/KEM.813.376.
[56] T. Schmidt, H. Assadi, F. Gärtner, H. Richter, T. Stoltenhoff, H. Kreye, T. Klassen, From particle acceleration to impact and bonding in cold spraying, J. Therm. Spray Technol. 18 (2009) 794–808, https://doi.org/10.1007/s11666-009-9357-7.